Dynamic Rheological Properties of High-Density Polyethylene/Polystyrene Blends Extruded in the Presence of Ultrasonic Oscillations

Guangshun Chen, Shaoyun Guo, Yuntao Li

State Key Laboratory of Polymer Materials Engineering, Polymer Research Institute of Sichuan University, Chengdu 610065, China

Received 25 February 2003; accepted 7 January 2004

ABSTRACT: The linear rheological properties of high-density polyethylene (HDPE), polystyrene (PS), and HDPE/PS (80/20) blends were used to characterize their structural development during extrusion in the presence of ultrasonic oscillations. The master curves of the storage shear modulus (G') and loss shear modulus (G'') at 200°C for HDPE, PS, and HDPE/PS (80/20) blends were constructed with time–temperature superposition, and their zero shear viscosity was determined from Cole–Cole plots of the out-of-phase viscous component of the dynamic complex viscosity (η'') versus the dynamic shear viscosity. The experimental results showed that ultrasonic oscillations during extrusion reduced G' and G'' as well as the zero shear viscosity of HDPE and PS because of their mechanochemical degradation in the presence of ultrasonic oscillations; this was confirmed by molecular weight measurements. Ultrasonic oscillations increased the slopes of log G' versus log G'' for HDPE and PS in the low-frequency terminal zone because of the increase in their molecular weight distributions. The slopes of log G' versus log G'' for HDPE/PS (80/20) blends and an emulsion model were used to characterize the ultrasonic enhancement of the compatibility of the blends. The results showed that ultrasonic oscillations could reduce the interfacial tension and enhance the compatibility of the blends, and this was consistent with our previous work. © 2004 Wiley Periodicals, Inc. J Appl Polym Sci 92: 3153–3158, 2004

Key words: rheology; blends

INTRODUCTION

Blending is a very important route for developing innovative materials with unique property combinations.[1,2] It has been increasingly recognized that interfacial adhesion and morphology control in multiphase polymer blends play important roles in the overall performance,[3,4] including the rheological properties. Depending on the structure and the nature of the dispersed phase, a wide spectrum of material properties can be tailored. The morphology of polymer blends not only depends on the thermodynamic properties of the components in the blends but also is mainly controlled by the deformation history (rheology) during mechanical melt blending. Understanding and quantifying, whenever possible, the relationships between the morphology and rheology is, therefore, essential for assessing and controlling the pertinent parameters for optimizing the processing conditions of these blends. The rheology of polymer blends has received a lot of attention because of its technological importance in polymer processing as well as theoretical reasons.

The rheological behavior of multiphase polymer blends has been studied extensively, both experimentally and theoretically.[5] The viscoelastic property of blends generally shows an increase in elasticity at low frequencies and very long relaxation times. Hietaoja et al.[6] studied the effect of the viscosity ratio on the phase inversion of polyamide 66/polypropylene blends. The impact strength appeared to critically depend on the continuous phase. Fortelny and Kovar[7] investigated the effect of the composition and properties of the components on the phase structure of polymer blends. Pressure effects in polymer melt rheology were discussed by Driscoll and Bogue,[8] who found that both the elastic modulus and the time constant depend on the pressure. Larson[9] reviewed the flow-induced mixing, demixing, and phase transitions in polymeric fluids. The viscosity–morphology–compatibility relationship of polymer blends was investigated by Chu et al.[10] They found that the viscosity of polyblends is related to the compatibility and composition of the two phases in the blend, and they explained the rheological behavior of polyblends from the viewpoints of morphology and compatibility.

Correspondence to: S. Guo (nic7702@scu.edu.cn).

Contract grant sponsor: Special Funds for Major State Basic Research Projects of China; contract grant number: G1999064800.

Contract grant sponsor: National Natural Science Foundation of China; contract grant number: 20374037 and 50233010.

Contract grant sponsor: State Education Ministry of China.

Journal of Applied Polymer Science, Vol. 92, 3153–3158 (2004)

TABLE I
Sample Codes and Preparation Conditions

Sample code	Sample	Repeated extrusion number	Ultrasound intensity, (W)	
			First extrusion	Second extrusion
H0	HDPE	1	0	—
H2	HDPE	1	200	—
S0	PS	1	0	—
S2	PS	1	200	—
HS0	HDPE/PS (80/20)	1	0	—
HS2	HDPE/PS (80/20)	1	200	—
HS00	HDPE/PS (80/20)	2	0	0
HS11	HDPE/PS (80/20)	2	100	100

For these studies, small-amplitude oscillatory shear tests are powerful tools, generating interesting information about the initial rheological and morphological properties of blends. Many researchers have expended great efforts to establish theories and models to theoretically describe and predict the macroscopic properties of blends in terms of the component properties.[11–14] Recently, an emulsion model has been used frequently.[15–19] It can be used to predict the dynamic modulus of blends with good results.

In our previous work,[20–22] ultrasonic oscillations were induced in an extruder. The experimental results showed that ultrasonic oscillations could remarkably improve the processing behavior of polystyrene (PS), linear low-density polyethylene (LLDPE), and high-density polyethylene (HDPE)/PS blends and inhibit the unstable flow of PS and LLDPE. Ultrasonic oscillations can greatly enhance the compatibility of HDPE/PS blends and cause a great reduction of the particle size of the dispersed phase. The morphology development of HDPE/PS blends in the presence of ultrasonic oscillations can certainly cause a change in the linear rheological behavior. In this work, we report some of the relationship between the linear viscoelastic behavior and morphology for HDPE/PS blends subjected to extrusion in the presence of ultrasonic oscillations. The emulsion model is used to explain our experimental results.

EXPERIMENTAL

Materials and sample preparation

The materials used were HDPE pDGDA6098; melt-flow index = 0.1 g/10 min, number-average molecular weight (M_n) = 3.18×10^4, and polydispersity = 8.8], supplied by Qilu Petrochemical Co., Ltd., (Linzi, China), and common-grade PS (M_n = 7.34×10^4 and polydispersity = 4.9), supplied by Nanjing Plastic Factory (Nanjing, China).

HDPE, PS, and a typical example of an HDPE/PS (80/20) blend were extruded in a special ultrasonic oscillation extruder developed in our laboratory, as described in refs. 20–22, in the presence of ultrasonic oscillations and in the absence of ultrasonic oscillations, and then they were pelletized. The screw rotation speed was 10 rpm, and the temperatures from the hopper to the die were 160, 180, 210, and 210°C. The sample codes are listed in Table I.

Measurements and characterization

The morphology of the blend was examined with an X-650 scanning electron microscope (Hitachi Co., Japan). Scanning electron microscopy (SEM) observations were made of the impact fracture surfaces at the temperature of liquid nitrogen. Gold was sputtered on the surfaces before the SEM observations. SEM micrographs of HDPE/PS (80/20) were analyzed with a Bencher digital image processing system to obtain the dispersed particle size in the blend.

For the rheological behavior, the samples were compression-molded at 200°C into disks 25 mm in diameter and about 1.5 mm thick. A 2ARES-9A rheometer (Rheometrics Co., USA) with parallel-plate geometry was used to measure the dynamic viscoelastic properties of HDPE, PS, and HDPE/PS (80/20) blends. The measurements were performed in a frequency range of 0.01–100 Hz between 170 and 220°C. The measurements were performed in a nitrogen atmosphere to avoid premature thermal degradation of the samples. The strain values were kept within the linear region.

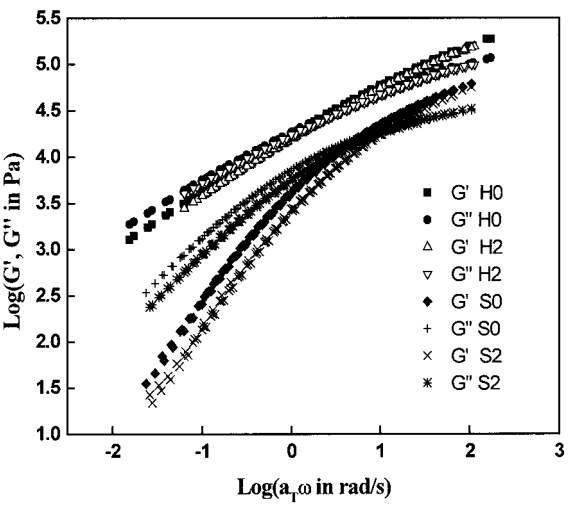

Figure 1 Master curves of G' and G'' at 200°C for H0, H2, S0, and S2.

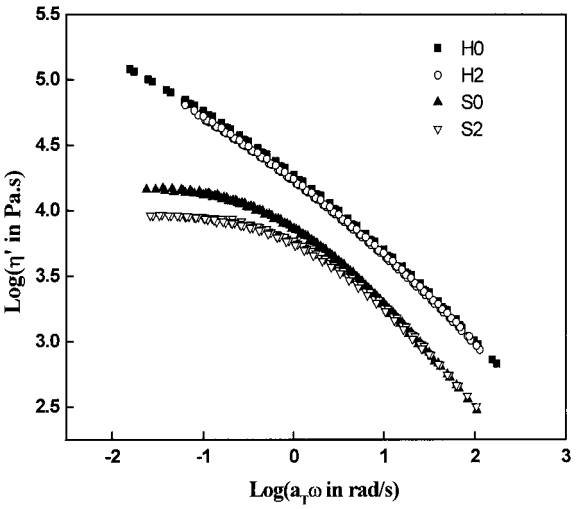

Figure 2 η' at 200°C for H0, H2, S0, and S2.

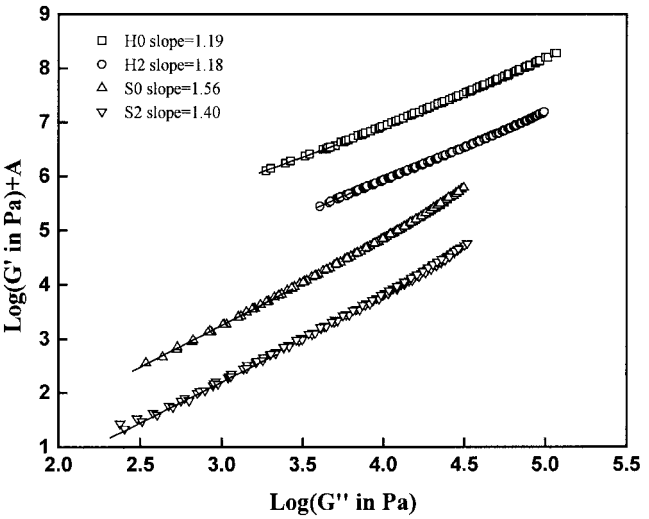

Figure 3 Plots of log G' versus log G'' for HDPE and PS at 200°C (H0, $A = 3$; H2, $A = 2$; S0, $A = 1$; and S2, $A = 0$).

RESULTS AND DISCUSSION

Effect of ultrasonic oscillations on the linear viscoelastic properties of HDPE and PS

The master curves of the storage shear modulus (G') and loss shear modulus (G'') at 200°C for HDPE and PS are shown in Figure 1. The G' and G'' values of HDPE (H2) and PS (S2) extruded in the presence of ultrasonic oscillations with an ultrasonic intensity of 200 W are lower than those of corresponding HDPE (H0) and PS (S0) extruded in the absence of ultrasonic oscillations. The dynamic shear viscosity (η') at 200°C of H2 and S2 is also lower than that of the H0 and S0 samples, especially at a low-frequency region (Fig. 2). The zero shear viscosity (η_0) was determined from Cole–Cole plots of η'' versus η', and the data are listed in Table II. η_0 for HDPE and PS extruded in the presence of ultrasonic oscillations decreases, and this indicates that the permanent change in the molecular structures of HDPE and PS occurs during extrusion in the presence of ultrasonic oscillations. Ultrasonic oscillations during extrusion cause the mechanochemical degradation of HDPE and PS. The decrease in the molecular weights of HDPE and PS extruded in the presence of ultrasonic oscillations (Table II) also confirms the permanent change in the molecular structures of HDPE and PS.

TABLE II
η_0 of the Samples at 200°C and M_n of HDPE and PS

Sample code	η_0 (Pa S)	$M_n \times 10^{-4}$	MWD
H0	1.7×10^5	2.81	8.19
H2	1.2×10^5	1.50	16.38
S0	1.5×10^4	7.34	4.90
S2	9.8×10^3	4.45	6.20
HS0	1.7×10^5		
HS2	1.6×10^5		
HS00	1.7×10^5		
HS11	1.1×10^5		

According to the linear viscoelastic theory,[23] in the terminal frequency zone ($\omega \to 0$), the dynamic viscoelastic functions are as follows:

$$G'(\omega)|_{\omega \to 0} = \omega^2 \int_{-\infty}^{+\infty} H(\tau)\tau^2 \, d \ln \tau = J_c^0 \, \eta_0^2 \, \omega^2 \qquad (1)$$

$$G''(\omega)|_{\omega \to 0} = \omega \int_{-\infty}^{+\infty} H(\tau)\tau d \ln \tau = \eta_0 \, \omega \qquad (2)$$

where $H(\tau)$ is the relaxation spectrum, τ is the relaxation time, and J_c^0 is the steady-state compliance. With

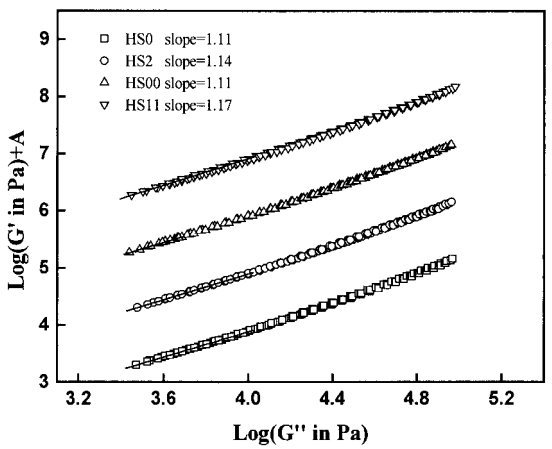

Figure 4 Plots of log G' versus log G'' for HDPE/PS (80/20) blends at 200°C (HS0, $A = 0$; HS2, $A = 1$; HS00, $A = 2$; and HS11, $A = 3$).

these equations, we can obtain three important relationships for the dynamic viscoelastic functions in the terminal frequency zone ($\omega \to 0$):

$$\log G'' \propto \log \omega, \quad \log G' \propto 2 \log \omega, \quad \log G' \propto 2 \log G'' \tag{3}$$

These relationships in the terminal frequency zone ($\omega \to 0$) show that the slope of log G' versus log G'' tends to the theoretical value of 2 for compatible polymer blends and polymers with narrow molecular weight distributions (MWDs). As shown in Figure 3, the slopes of log G' versus log G'' for H2 and S2 are lower than those for corresponding H0 and S0, and this indicates that ultrasonic oscillations during extrusion cause increases in MWDs of HDPE and PS (Table II).

Effect of ultrasonic oscillations on the linear viscoelastic properties of HDPE/PS (80/20) blends

Terminal zone properties

Because dynamic viscoelastic properties are very sensitive to variations in the morphological state of multicomponent/multiphase polymer systems (e.g., immiscible polymer blends, microphase-separated block copolymers, and liquid-crystalline polymers),[1,24–28] we can obtain valuable information about the compatibility and phase separation of polymer blends by testing their dynamic viscoelastic properties, which cannot be obtained by common methods. In the long-relaxation-time (or low-frequency) range, the dynamic viscoelastic properties are linear with variations in the stress, and the stress on polymer blends under this condition is so small that the morphological state of the polymer blends remains almost unchanged. Meanwhile, the logarithm relationship between G' and G'' shows temperature independence; the relationship is very sensitive to variations in the morphology of blends. We can find some phase-separation information for polymer blends by understanding the relationship between log G' and log G''.

The relationship between log G' and log G'' of HDPE/PS (80/20) blends is shown in Figure 4. Ultrasonic oscillations during the extrusion of the polymer blends cause an increase in the slope of log G' versus log G'' in the low-frequency range, and this indicates that the particle size and particle size distribution of the dispersed phase decrease and the compatibility of HDPE/PS blends is improved during extrusion in the presence of ultrasonic oscillations. This is consistent with our previous work.[22]

Calculation of the interfacial tension (α) with the emulsion model

Some reports[11,14–18] have proposed an emulsion model for polymer blend systems that takes α into account. This model has been used to estimate α and interpret some experimental results. After this section, we use it to estimate α values of HDPE/PS (80/20) blend systems.

Palierne[11] proposed an emulsion-type model including the viscoelasticity of the phases, hydrodynamic interactions, and the effect of α. In this model, the systems are considered emulsions of viscoelastic incompressible materials, in which the droplets forming the dispersed phase are spherical in equilibrium. The main assumption leading to the constitutive equation of the emulsion is that the droplet deformation remains small. If α between the matrix and the dispersed phase is assumed to be independent of the local shear and variation of the interfacial area, the following simplified expression for the complex shear modulus (G^*) of the emulsion can be obtained:

$$G_b^*(\omega) = G_M^*(\omega) \frac{1 + 3\sum_i \Phi_i H_i(\omega)}{1 - 2\sum_i \Phi_i H_i(\omega)} \tag{4}$$

where

$$H_i(\omega) = \frac{\begin{array}{l} 4(\alpha/R_i)[2G_M^*(\omega) + 5G_I^*(\omega)] + \\ [G_I^*(\omega) - G_M^*(\omega)][16G_M^*(\omega) + 19G_I^*(\omega)] \end{array}}{\begin{array}{l} 40(\alpha/R_i)[G_M^*(\omega) + G_I^*(\omega)] + \\ [2G_I^*(\omega) + 3G_M^*(\omega)][16G_M^*(\omega) + 19G_I^*(\omega)] \end{array}} \tag{5}$$

$G_b^*(\omega)$, $G_M^*(\omega)$, and $G_I^*(\omega)$ are the complex shear moduli for the blend, matrix, and inclusion, respectively. R_i is the droplet radius, and Φ_i is the volume fraction of droplets with radius R_i. The summation is carried out over the distribution of droplets sizes. For narrow distributions, a good agreement between the model prediction and experimental data can be obtained.

For our experiments, we have assumed that α does not vary with the deformation, and we have used the volume-average particle radius (R) and total volume fraction (Φ) of PS in HDPE/PS (80/20) blends to replace the distribution particle size and volume fraction, respectively. Therefore, we could use eqs. (4) and (5) to estimate α values for blends extruded with and without ultrasonic oscillations.

If G' and G'' of the components, the particle size, and α are known, the dynamic storage modulus of the blend (G_b') and dynamic loss modulus of the blend (G_b''), with a uniform particle size distribution, can be easily calculated with eqs. (4) and (5). The expressions are as follows:

$$G_b' = \frac{1}{D}[G_M'(B_1B_2 + B_3B_4) - G_M''(B_1B_4 - B_2B_3)] \tag{6a}$$

$$G_b'' = \frac{1}{D}[G_M'(B_1B_4 - B_2B_3) + G_M''(B_1B_2 + B_3B_4)] \tag{6b}$$

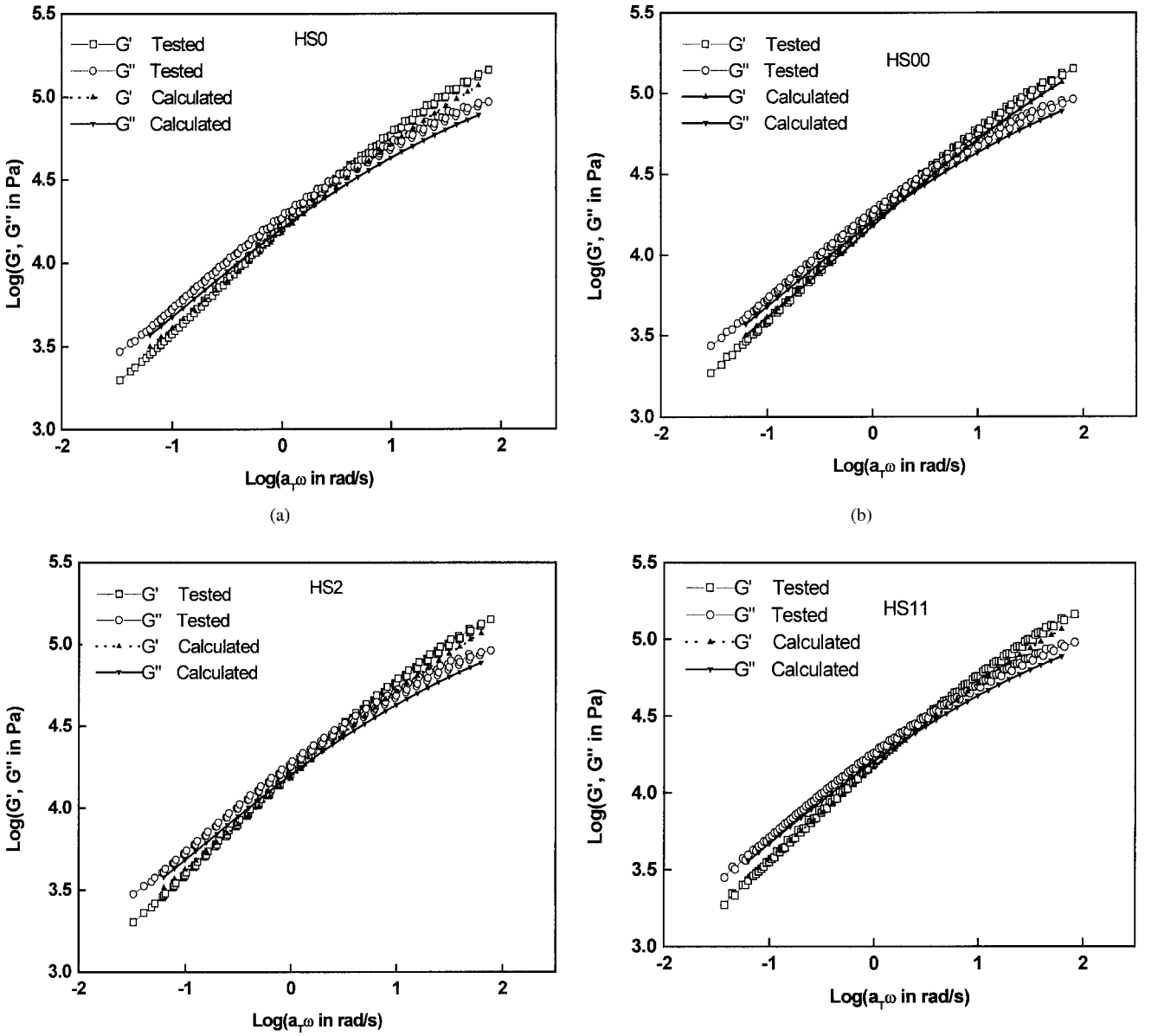

Figure 5 Comparison of the tested and calculated data for (a) HS0, (b) HS00, (c) HS2, and (d) HS11 at 200°C

where

$$B_1 = C_1 - 2\Phi C_3, \quad B_2 = C_1 + 3\Phi C_3, \quad B_3 = C_2 - 2\Phi C_4, \quad B_4 = C_2 + 3\Phi C_4, \quad D = B_1^2 + B_3^2 \quad (7)$$

C_1, C_2, C_3, and C_4 are obtained with the following equations:

$$C_1 = 40\left(\frac{\alpha}{R}\right)(G'_M + G'_I) + 38(G'^2_I - G''^2_I) + 48(G'^2_M - G''^2_M) + 89(G'_M G'_I - G''_M G''_I) \quad (8a)$$

$$C_2 = 40\left(\frac{\alpha}{R}\right)(G''_M + G''_I) + 96G'_M G''_M + 76G'_I G''_I + 89(G'_M G''_I + G''_M G'_I) \quad (8b)$$

$$C_3 = 4\left(\frac{\alpha}{R}\right)(2G'_M + 5G'_I) - 16(G'^2_M - G''^2_M) + 19(G'^2_I - G''^2_I) - 3(G'_M G'_I - G''_M G''_I) \quad (8c)$$

$$C_4 = 4\left(\frac{\alpha}{R}\right)(2G''_M + 5G''_I) - 32G'_M G''_M + 38G'_I G''_I - 3(G'_M G''_I + G''_M G'_I) \quad (8d)$$

G'_M and G'_I are the dynamic storage moduli and G''_M, and G''_I are the dynamic loss moduli for the matrix and inclusion, respectively. With G'_M, G'_I, G''_M, and G''_I at the same frequencies, we can obtain G'_b and G''_b with eqs. (6)–(8). To obtain the best value of α, we compared the calculated values of G'_b and G''_b with experimental data until the value of J, defined by eq. (9), was minimized:

TABLE III
Calculated α Values and Tested R Values for HDPE/PS (80/20) Blends

Sample code	α (mN/m)	R (μm)
HS0	4.5	1.14
HS2	3.9	0.83
HS00	5.2	1.31
HS11	1.53	0.73

$$J = \sum_{i=1}^{n} \left\{ \left(\frac{G'_{\text{exp},i} - G'_{\text{calc},i}}{G'_{\text{exp},i}} \right)^2 + \left(\frac{G''_{\text{exp},i} - G''_{\text{calc},i}}{G''_{\text{exp},i}} \right)^2 \right\} \quad (9)$$

where $G'_{\text{exp},i}$ and $G''_{\text{exp},i}$ are the experimental moduli and $G'_{\text{calc},i}$ and $G''_{\text{calc},i}$ are the calculated moduli for the blends.

The master curves of G' and G'' at 200°C for an HDPE/PS (80/20) blends and their model predictions are shown in Figure 5. The values of α and R are listed in Table III. The α values of the blends decrease if the blends are extruded in the presence of ultrasonic oscillations. For blends extruded twice with an ultrasonic intensity of 100 W, α decreases remarkably. This confirms the ultrasonic improvement of the compatibility for the blends, as our previous article described.[22] For HS11, the value of 1.53 mN/m is similar to that of the PS/polyethylene (PE)/styrene-*co*-ethylene-butene random copolymer (SEBS) blend system reported in refs. 17 and 19; SEBS is a modifier agent for the PS/PE blend system. Therefore, the reduction of both α and the particle size of the blends confirms the enhancement of the compatibility of the blends extruded in the presence of ultrasonic oscillations.

CONCLUSIONS

The linear rheological properties of HDPE, PS, and HDPE/PS (80/20) blends have been used to characterize their structural development during extrusion in the presence of ultrasonic oscillations. Ultrasonic oscillations can reduce the dynamic shear moduli for HDPE, PS, and HDPE/PS (80/20) blends as well as their zero-shear viscosities because of their mechanochemical degradation in the presence of ultrasonic oscillations.

The slopes of log G' versus log G'' for HDPE/PS (80/20) blends and an emulsion model have been used to characterize the ultrasonic enhancement of the compatibility of the blends. Ultrasonic oscillations reduce α and the particle size of HDPE/PS (80/20) blends and improve their compatibility.

References

1. Polymer Alloys and Blends; Utracki, L. A., Ed.; Hanser: Munich, 1990; p 13.
2. Chiu, W.; Fang, S. J Appl Polym Sci 1985, 30, 1473.
3. Zhang, Z. L.; Zhang, H. D.; Yang, Y. L.; Vinckier, I.; Laun, H. M. Macromolecules 2001, 34, 1416.
4. Cassu, S. N.; Felisberti, M. I. J Appl Polym Sci 2001, 82, 2514.
5. Manchado, M. A. L.; Biagiotti, J.; Kenny, J. M. J Appl Polym Sci 2001, 81, 1.
6. Hietaoja, P. T.; Holsti-Miettinen, R. M.; Seppala, J. V.; Ikkala, O. T. J Appl Polym Sci 1994, 54, 1613.
7. Fortelny, I.; Kovar, J. Eur Polym J 1992, 28, 85.
8. Driscoll, P. D.; Bogue, D. C. J Appl Polym Sci 1990, 39, 1755.
9. Larson, R. G. Rheol Acta 1992, 31, 497.
10. Chu, L.-H.; Guo, S.-H.; Chiu, W.-Y.; Tseng, H.-C. J Appl Polym Sci 1993, 40, 1791.
11. Palierne, J. F. Rheol Acta 1990, 29, 204.
12. Lee, H. M.; Park, O. O. J Rheol 1994, 38, 1405.
13. Scholz, P.; Froelich, D.; Muller, R. J Rheol 1989, 33, 481.
14. Gramespacher, H.; Meissner, J. J Rheol 1992, 36, 1127.
15. Graebling, D.; Muller, R.; Palierne, J. F. Macromolecules 1993, 26, 320.
16. Bousmina, M.; Muller, R. J Rheol 1993, 37, 663.
17. Bousmina, M.; Bataille, P.; Sapieha, S.; Schreiber, H. P. J Rheol 1995, 39, 499.
18. Friedrich, C.; Gleinser, W.; Korat, E.; Maier, D.; Weese, J. J Rheol 1995, 39, 1411.
19. Mekhilef, N.; Carreau, P. J.; Favis, B. D.; Martin, P.; Ouhlal, A. J Polym Sci Part B: Polym Phys 2000, 38, 1359.
20. Chen, G.; Guo, S.; Li, H. J Appl Polym Sci 2002, 84, 2451.
21. Guo, S.; Li, Y.; Chen, G.; Li, H. Polym Int 2002, 51, 1.
22. Chen, G.; Guo, S.; Li, H. J Appl Polym Sci 2002, 86, 23.
23. Ferry, J. D. Viscoelastic Properties of Polymers, 3rd ed.; Wiley: New York, 1980; p 56.
24. Han, C. D.; Kim, J. K. Polymer 1993, 12, 2533.
25. Yanovsky, Y. G. Polymer Rheology: Theory and Practice; Chapman & Hall: London, 1993; p 517.
26. Han, C. D.; Kim, J.; Kim, J. K. Macromolecules 1989, 22, 383.
27. Han, C. D.; Kim, J. J Polym Sci Part B: Polym Phys 1987, 25, 1741.
28. Qiang, Z.; Masaoki, T.; Toshiro, M. Chem J Chin Univ 1999, 20, 969.